VIBRATION ANALYSES OF RAILWAY SYSTEMS USING PROPOSED NEURAL PREDICTORS

S. Yildirim[*], *C. Sevim*[†], *M. Kalkat*[†]

Abstract: Due to travelling on railway systems; there are many gaps and problems in cross areas. Therefore; it is necessary and very important to establish intelligent crossing systems in such areas. On the other hand, it is not possible for trains to stop or brake immediately against an obstacle due to their high speed and inertia. For this reason, it is necessary to work on the safety/warning of the other main factors and necessities (pedestrians and vehicles) in level crossings. This experimental investigation is carried out by using an experimental real-time train and crossing systems. The main vibration parameters are analysed by using neural networks. First, the dynamics of the train-rail system related to level crossings are examined, and the vibrations created by the train on rails are measured at different speeds. Then three types of proposed neural networks predictors, Levenberg-Marquardt backpropagation (LMBP), scaled conjugate gradient backpropagation (SCGB) and BFGS quasi-Newton backpropagation (BFGS) are used to predict the vibration of the train-rail system. From the results, it is seen that the proposed LMBP is more suitable for analysing and predicting the vibration of the train-rail system. It is clear that the speeds of the trains approaching the level crossing can be estimated from the vibration of the trains on the rails.

Key words: *vibration analysis, railway systems, neural networks, prediction*

Received: March 15, 2021 **DOI:** 10.14311/NNW.2023.33.009
Revised and accepted: June 30, 2023

1. Introduction

With the increasing population in the world and the ever-evolving technology, advanced level fast and safe public transportation needs are also increasing. One of the most preferred types of transportation in the world is especially railway systems. For this reason, the railway networks that are becoming more common nowadays make the intersection of highway and railway unavoidable. Level crossings at the intersection of the highway and the railway are the sections of the railway systems that have the highest security flaw today. Although there are some studies to

[*]Sahin Yildirim – Corresponding author; Erciyes University, Faculty of Engineering, Turkey, E-mail: sahiny@erciyes.edu.tr

[†]Caglar Sevim; Menderes Kalkat; Nigde University, Faculty of Engineering, Turkey, E-mail: caglar.sevim@ohu.edu.tr, mkalkat@ohu.edu.tr

improve and develop level crossing systems in terms of security, these studies are still not sufficient. In particular, the number of uncontrolled level crossings is high compared to the controlled level crossings [1].

The main problem of existing level crossing systems is a large number of time losses in level crossings. In most of the level crossings, the gate barriers are closed and opened regardless of the train speed. Especially, the driver and pedestrians are impatient and somehow try to cross the level crossing, as the downtime of the gate is long. This causes major accidents to occur in level crossings. Therefore, it is necessary to develop a compact, safe and low-cost level crossing control system to cover all type of level crossings. However, there are also studies on the control of level crossing barriers and these studies have not been able to bring the level crossing safety to the desired level and the implementation of these studies requires high costs. Hence, these problems necessitate a search for a cheap and safe solution that covers all level crossing systems related to level crossings. Bahloul et al. [2] have suggested some technological solutions to improve safety at level crossings. They studied on the PANsafer project whose purpose is to improve safety at level crossings and carried out statistical analysis using accident/incident databases and studied on the human behaviour to determine potential risky situations. On the other hand, Burdzik and Nowak [3] simulated the working states that can potentially have an effect on the vibration environment of railway infrastructure. They listed the main frequencies for the dominant components of the signals and showed that it could be possible to separate the vibration properties of signals arising from different sources. Also, railway vibration was analysed using micro-electromechanical systems-type accelerometer sensor to recognise the existence and to measure the position of the train as a warning system by Ardiansyah et al. [4]. They used a neural network to recognise the vibration patterns of the both the train and the non-train and reported that the neural network can recognise the vibrations generated by the train to non-train with a 100% success rate at a distance of 45 meters. Larue et al. [5] conducted research on time losses that occurred at level crossings. In their research, they collected data on a selected level crossing to investigate what caused more time loss and found that warning times are the main issue of redundant level crossing downtime. The study showed that time loss in level crossings could be reduced with some improvements. Sharad et al. [6] studied on an early warning system on unmanned level crossings. The system is based on embedded systems with some sensors (pressure, vibration, magnetic and proximity) and communications. Sensors are supported by a laser beam to perceive the train. The laser beam is the first sign for the upcoming train, and the other sensors help to detect the train pass. Another study on the safety of level crossing was made by Edle et al. [7]. They studied on the multilevel automated security system which aims to unmanned level crossings. The system has three security levels: GPS system, IR and RFID systems, and IR sensors on the level crossing gate. Mainly, the GPS system sends data to the control unit about the velocity and the position of the train. Intercalarily, despite GPS faults due to weather conditions, IR-RFID system support the security system. The system also detects whether there is a vehicle or someone in the gate and provides time to take precautions by the driver. However, Mahdi and Zuhairi [8] designed a simple level crossing control system based on IR LED-sensor system. If the train crosses the sensor, the sensor provides a signal to the micro-controller, and the micro-controller closes the gate if the gate is open. When the train is passed the second sensor, the gate will re-open by the micro-controller. Kiruthiga et al. [9] have developed a system based on the obstacle sensor and GSM modem to prevent casualties and train crashes. Mostafa et al. [10] improved a radio-based intelligent level crossing system. They use radio transmitters at the head and end of the train. The controller gets information about the train when the train passes through a sensor and control the gate. Another sensor-based study made by Biswas et al. [11]. When the train passes through an IR sensor, the controller of the level crossing activates warning systems and starts closing the gate. When the gate is closed at 45 degrees, the system checks whether there is a vehicle or anything else in the level crossing by means of the pressure sensors on both sides of the level crossing. If there is no vehicle in the level crossing, the gate continues to close. If there is a vehicle in the level crossing, the control unit does not close the gate barriers for a while and allows the vehicle to pass and warns the train driver. Ameen [12] have studied on the vibration-based early stimulation system regardless of the train speed for track signalling of level crossings. The goal of the study is a low-cost system for unattended level crossings. The system is based on a piezo vibration sensor and Arduino controller board. When a train passes over the sensor at any speed, the vibration sensor sends a signal to the controller board; thus, the signal system starts to give information about the train. Kitamura et al. [13] carried out a study with autonomous decentralised technology on level crossing systems. A network level crossing system was experimentally applied to reduce the influence of level crossings failure. Another purpose of the system is to continue controlling the system without interruption and loss of time in case of a possible error. Burdzik et al. [14] conducted an experimental study on vibration analysis of wheel-rail contact. They measured the 3-axle distribution of vibration generated by the train simulator wheel-rail contact and analysed it through basic statistics and Fourier transformations to determine the dominant frequency bands.

If the studies conducted are examined, it can be seen that, until now, for level crossings, the application area of the solution suggestions is limited and high cost. Today, it confirms this phenomenon the fact that the number of uncontrolled level crossings is still high. However, artificial neural networks are low-cost systems that have a wide range of applications and provide reliable results. A level crossing system to be controlled with neural networks will be both compact and cost-effective. As far as the authors are known, there is no investigation such as this work. This paper presents a proposed investigation on intelligent level crossing system design and analyses with sensor and control technology. In accordance with this purpose; three types of artificial neural networks were used to analyse and evaluate vibration resulting from train-rail influences under different operating speeds. The vibration data were experimentally obtained by means of vibration sensors placed on the railway system.

The paper is organised as follows: Section 2 describes the motion equation of railway systems. Section 3 explains the experimental system. Section 4 gives some information about the proposed neural network. Results from experimental analyses and neural networks are given in Section 5. The study is accomplished with conclusions and discussion in Section 6.

2. Description of dynamic of railway structure

In order to better understand the vibration analysis of the wagon-rail system, it is necessary to obtain the equations of motion of the system. There are many studies on this subject in the literature [15–18]. Mass models, continuous models and finite element models are the most used models for railway vehicles. In the wagon-rail dynamics, the most critical point is the interaction between the wheel and rail. There are different approaches to model this interaction in the literature [19–26].

In this study, the components in the train-rail system whose vibration is measured consist of wagon, bogie, wheel, rail, sleepers and ballasts, and dynamic equations are derived according to these expressions. Quarter wagon system is taken into account as it reflects the general behaviour when obtaining dynamic equations. Dynamic system model of train-rail is given in Fig. 1. If the motion equation is created for the wagon body, here m_{v} shows the wagon mass, m_{b} bogie mass, m_{w} wheel mass and the suspension stiffness coefficient between the wagon and bogie is defined by k_{bv}. Generally, leaf springs are used between bogies and wheels, and their stiffness is defined by k_{wb}. Therefore, the motion equation for the wagon body (Eq. (1)) and the motion equation for the bogie (Eq. (2)) are defined below

$$m_{\mathrm{v}}\ddot{y}_{\mathrm{v}} + k_{\mathrm{bv}}y_{\mathrm{v}} - k_{\mathrm{bv}}y_{\mathrm{b}} = 0, \tag{1}$$

$$m_{\mathrm{b}}\ddot{y}_{\mathrm{b}} + k_{\mathrm{wb}}\left(y_{\mathrm{b}} - y_{\mathrm{w}}\right) + k_{\mathrm{bv}}\left(y_{\mathrm{b}} - y_{\mathrm{v}}\right) = 0. \tag{2}$$

Due to the bogie is attached to the wagon at the centre of the bogie and have one wheel, the pitch motion of the bogie is neglected. A detailed view of the bogie is given in Fig. 2.

Equation of motion for the wheel

$$m_{\mathrm{w}}\ddot{y}_{\mathrm{w}} + k_{\mathrm{wb}}\left(y_{\mathrm{w}} - y_{\mathrm{b}}\right) + F(t) = 0, \tag{3}$$

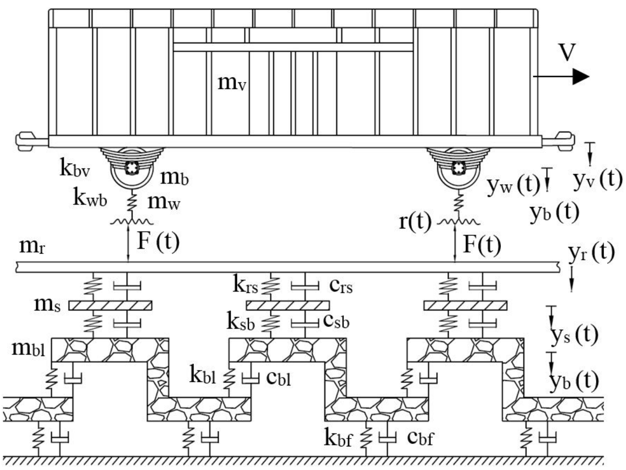

Fig. 1 *Schematic representation of train-rail dynamic system model.*

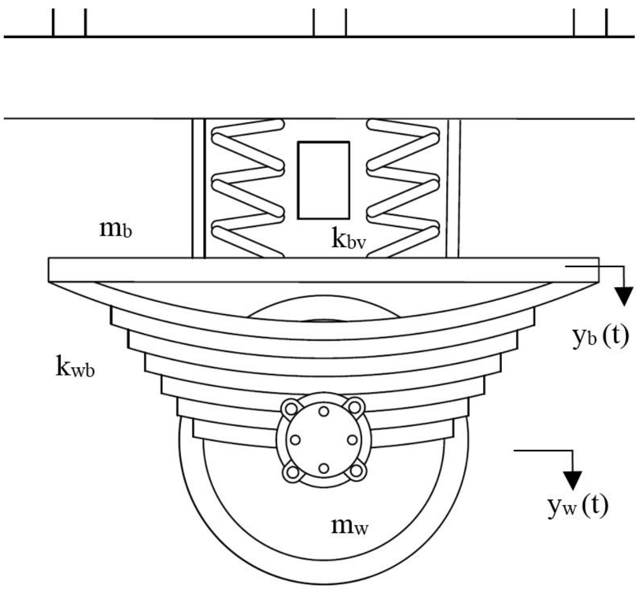

Fig. 2 *Schematic view of the bogie structure.*

can be written. Here y_{w} is the weight of the wheel, $F(t)$ is the contact force caused by wheel-rail contact. If the wheel-rail contact force is written according to the Hertzian contact theory, depending on the wheel, bogie and wheel surface deformation and a specific Hertzian contact coefficient [20, 21]

$$F(t) = C_{\mathrm{H}}[y_{\mathrm{w}}(t) - y_{\mathrm{r}}(t) - r(t)]^{3/2}. \tag{4}$$

Here C_{H} is a Hertzian coefficient depending on the wheel-rail contact, and $r(t)$ is a wheel surface function. And so, with taking into account the static forces, the total vertical forces

$$F^{*}(t) = F(t) + [0.5\,(m_{\mathrm{v}} + m_{\mathrm{b}}) + m_{\mathrm{w}}]\,g. \tag{5}$$

Sleepers are one of the main components which in the use of concrete nowadays, rarely in wood form, and are both supporting and keeping line the rail. The force generated between each sleeper-rail can be defined as follows

$$F_{\mathrm{rt}(i)}(t) = k_{\mathrm{rs}(i)}\left[y_{\mathrm{r}}\left(x_i, t\right) - y_{\mathrm{s}(i)}(t)\right] + c_{\mathrm{rs}(i)}\left[\dot{y}_{\mathrm{rs}(i)}\left(x_i, t\right) - \dot{y}_{\mathrm{s}(i)}(t)\right], \tag{6}$$

where x_i is the position of ith sleeper. $k_{\mathrm{rs}(i)}$ and $c_{\mathrm{rs}(i)}$ are the stiffness and damping coefficients between the rail and sleepers, respectively. Ballast layer has a significant effect on reducing the impact of vibration on the ground by damping. The vibration arising from the wheel-rail interaction is transmitted from the rails to the sleepers and then from the sleepers to the ballasts. In addition, considering the interactions of ballasts among themselves, the equations of motion for traverses and ballasts are given in Eq. (7) and Eq. (8).

$$
\begin{aligned}
& m_{\mathrm{s}(i)} \ddot{y}_{\mathrm{s}(i)}(t)+\left(c_{\mathrm{rs}}+c_{\mathrm{sb}}\right) \dot{y}_{\mathrm{s}(i)}(t)+\left(k_{\mathrm{rs}}+k_{\mathrm{sb}}\right) y_{\mathrm{s}(i)}(t)-c_{\mathrm{sb}} \dot{y}_{\mathrm{sb}(i)}(t) \\
& \quad-k_{\mathrm{sb}} y_{\mathrm{sb}(i)}(t)-c_{\mathrm{rs}} \sum_{k=1}^{K} Y_k\left(x_i\right) \dot{t}_k(t)-k_{\mathrm{rs}} \sum_{k=1}^{K} Y_k\left(x_i\right) t_k(t)=0 \\
& \qquad i=1,\ 2, \ldots, N,
\end{aligned} \tag{7}
$$

$$
\begin{aligned}
& m_{\mathrm{b}(i)} \ddot{y}_{\mathrm{b}(i)}(t)+\left(c_{\mathrm{sb}}+c_{\mathrm{bf}}+2 c_{\mathrm{bl}}\right) \dot{y}_{\mathrm{b}(i)}(t)+\left(k_{\mathrm{sb}}+k_{\mathrm{bf}}+2 k_{\mathrm{bl}}\right) y_{\mathrm{b}(i)}(t) \\
& -c_{\mathrm{sb}} \dot{y}_{\mathrm{s}(i)}(t)-k_{\mathrm{sb}} y_{\mathrm{s}(i)}(t)-c_{\mathrm{bl}} \dot{y}_{\mathrm{b}(i+1)}(t)-k_{\mathrm{bl}} y_{\mathrm{b}(i+1)}(t)-c_{\mathrm{bl}} \dot{y}_{\mathrm{b}(i-1)}(t) \\
& \qquad -k_{\mathrm{bl}} y_{\mathrm{b}(i-1)}(t)=0 \\
& \qquad i=1,\ 2, \ldots, N,
\end{aligned} \tag{8}
$$

where Y_k is kth deflection mode and t_k is the time coordinate. k_{sb} and c_{sb} are the stiffness and damping coefficients between sleeper and ballast, respectively. k_{bl} and c_{bl} are the stiffness and damping coefficient of the interaction between the ballast layer. k_{bf} and c_{bf} as to are the stiffness and damping coefficients of the interaction between ballast and ground.

The force between the ballast layer and the sleepers can be expressed as follows

$$
\begin{aligned}
F_{\mathrm{sb}(i)}(t) = \; & k_{\mathrm{sb}(i)}[y_{\mathrm{s}(i)}(t)-y_{\mathrm{b}(i)}(t)]+c_{\mathrm{sb}(i)}[\dot{y}_{\mathrm{s}(i)}(t)-\dot{y}_{\mathrm{b}(i)}(t)] \\
& +k_{\mathrm{bl}(i)}[y_{\mathrm{b}(i)}(t)-y_{\mathrm{b}(i+1)}(t)]+c_{\mathrm{bl}(i)}[\dot{y}_{\mathrm{b}(i)}(t)-\dot{y}_{\mathrm{b}(i+1)}(t)] \\
& +k_{\mathrm{bl}(i)}[y_{\mathrm{b}(i)}(t)-y_{\mathrm{b}(i-1)}(t)]+c_{\mathrm{bl}(i)}[\dot{y}_{\mathrm{b}(i)}(t)-\dot{y}_{\mathrm{b}(i-1)}(t)]
\end{aligned} \tag{9}
$$

Thus, the motion equation of the entire system can be written as follows, with the rail being regarded as the Euler beam.

$$
\begin{aligned}
EI \frac{\partial^4 y_{\mathrm{r}}(x, t)}{\partial x^4}+m_{\mathrm{r}} \frac{\partial^2 y_{\mathrm{r}}(x, t)}{\partial t^2} = & -\sum_{i=1}^{N} F_{\mathrm{rs}(i)}(t) \delta(x-x_i) \\
& +\sum_{j=1}^{2} F^*(t) \delta\left(x-x_j\right),
\end{aligned} \tag{10}
$$

where N is the total number of sleepers considered. j is the number of combined wheel-sets in the wagon model representing the number of moving load points affecting the rail. E is the modulus of elasticity depending on the material of the rail, and I represents the second moment of inertia.

3. Experimental measurement system

In this section, the measurement method and measurement information of the vibration created by the train on the rails are given. Measurement was performed for train with three different speeds. Information of speeds of the train are given in Tab. I.

Measurement number	Speed [km/h]
1	40
2	52
3	60

Tab. I *Measurement performed train system information.*

The real-time measurement system is given in Fig. 3. Uni-axial acceleration sensors were used for vibration measurement and data from four vibration sensors was taken for each measurement at the same time.

Acceleration sensors are directly connected to the rail and the measurement process has started as the train approaches the sensor, and then is terminated when the train moves away and the vibration level decreases again. The system, which is measured vibration, consists of train body, bogie, rail, traverse and ballast layer.

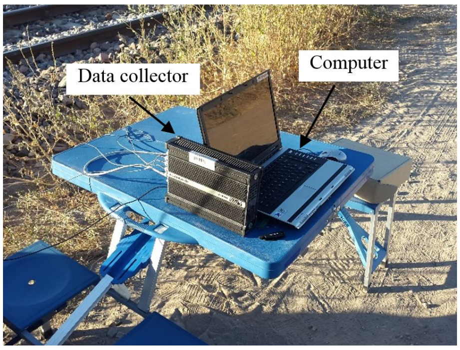

(a)

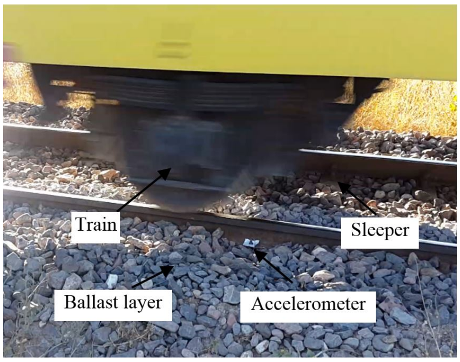

(b)

Fig. 3 *Real-time measurement system: (a) Data collection system. (b) Measurement system overview.*

4. The main proposed structure of artificial neural network

Artificial neural network systems are used by computer-aided softwares that operate in a structure which similar to the human perception and learning system and have the ability to process the information on their own.

Feedforward network structure is one of the essential classes of artificial neural networks because of its simple structure and stability. In general, the network structure consists of three main layers as the input layer, the hidden layer and the output layer. There may be more than one hidden layer level in the hidden layer region, depending on the data density and type [27].

In this study, an intelligent data acquisition system with (Bruel Kjaer 4524 B 001 type IDA) one-axial accelerometers and a computer were used to measure and analyse vibration.

The block diagram of the experimental setup used to collect the vibration data generated by the train on rails at three different speeds and weights are given in Fig. 4. Where i_m is measured data and i_n is neural networks acceleration values. These data were tested in the next stage for the prediction of train speed with

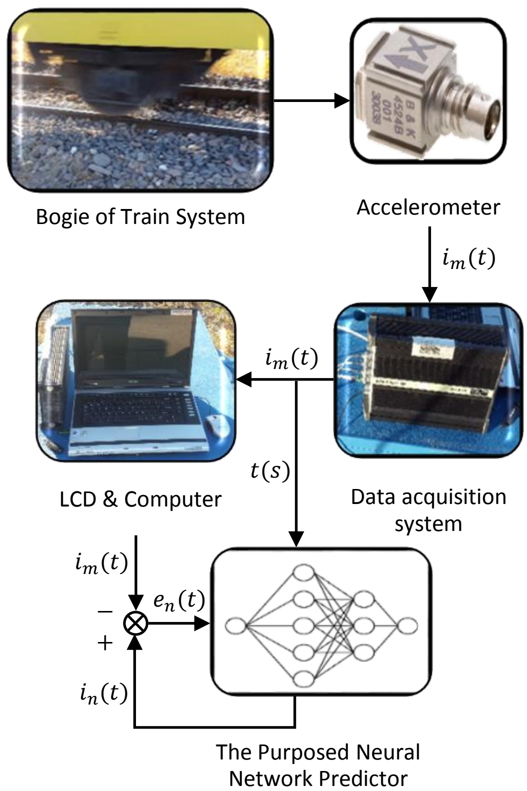

Fig. 4 *Experimental system and block diagram with NN predictor.*

three different learning algorithms via computer. 70% of the total data is used for training, 15% is used for testing, and 15% is used for validation. In order to improve the predictability of the model, test and validation data are randomly selected.

The radial based artificial neural network has a feedforward artificial neural network structure, like other feedforward artificial neural networks, it consists of the input layer, the hidden layer and the output layer as given in Fig. 5. Radial based neural network function

$$F(x) = \sum_{i=1}^{m} \omega_i \varphi_i(x), \tag{11}$$

where ω_i is the weight value between layers and x is the n-dimensional input vector. m is the number of neurons in the hidden layer. $\varphi_i(x)$ is the transfer function, where [27]

$$\varphi_i(x) = \exp\left(-\sum_{k=1}^{n} (x_k - c_{\mathrm{jk}})^2 r_{\mathrm{jk}}^2\right). \tag{12}$$

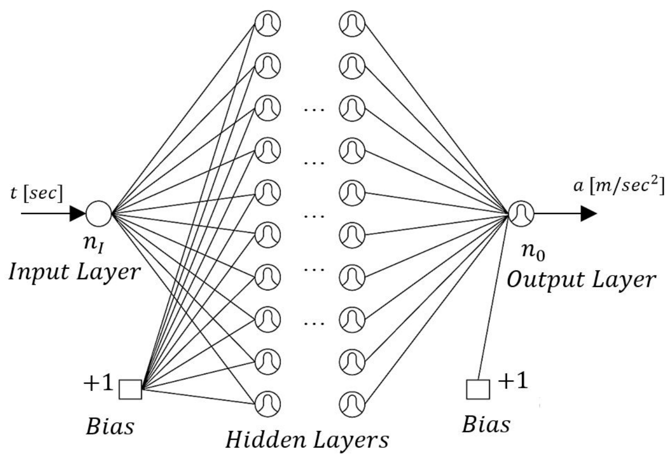

Fig. 5 *The structure of radial based ANN.*

4.1 Levenberg-Marquardt algorithm

Derived from Newton algorithms, the Levenberg-Marquardt algorithm is the minimum mean square error calculation method based on maximum neighbourhood. This algorithm consists of the best features of the Gauss-Newton and gradient-descent algorithms and removes the limitations of these two methods. In general, this method is not affected by the slow convergence problem and performs parameter update operations with the error vector and Jacobian matrix created for all inputs. Levenberg-Marquart algorithm, which is the combination of the Gauss-Newton algorithm, is more effective in optimisation problems than gradient descent algorithm. The Levenberg-Marquardt algorithm uses system resources (memory etc.) more than other algorithms, but the training of the network takes place in a shorter time. Training ends when generalisation stops recovery [28, 29].

$$\Delta\omega = \left(\mathbf{J}^{\mathrm{T}}\mathbf{J} + \mu\mathbf{I}\right)^{-1}\mathbf{J}^{\mathrm{T}}e, \tag{13}$$

where ω is the weight vector, $\mathbf{I}$ is a unit matrix and μ is a combination coefficient. $\mathbf{J}$ point out the Jacobian matrix in size $[(Pxn), N]$ and e point out error vector in size $[(Pxn), 1]$. Here P shows the number of training samples. n and N show the number of outputs and the number of weight, respectively.

4.2 BFGS quasi-Newton backpropagation

As an alternative to the generalised backpropagation algorithm, the Newtonian algorithm provides faster optimisation and is expressed in Eq. (14).

$$x_{k+1} = x_k - w_k^{-1} g_k. \tag{14}$$

w_k^{-1} is a Hessian matrix, which refers to quadratic derivatives of the defined performance index in the current values of weight and threshold values. Although the Newton method converges faster than the conjugate gradient algorithm, the calculation of the Hessian matrix used for feedforward networks is quite difficult and time-consuming. On the basis of the Newtonian algorithm, methods that do not need to calculate the Hessian matrix have been developed. These methods are called quasi-Newton algorithms. The most successful method of quasi-Newton methods is the Broyden-Fletcher-Goldfarb-Shanno (BFGS) method. The BFGS method is based on the method of calculating the approximate value of the Hessian matrix at each iteration [30, 31].

$$p(t) = -w^{-1}(t)g(t), \tag{15}$$

$$w\,(t+1) = w(t) + \Delta w(t), \tag{16}$$

$$\Delta w(t) = \frac{g(t)g(t)^{\mathrm{T}}}{g(t)^{\mathrm{T}}p(t)} . \frac{\Delta g(t)\Delta g(t)^{\mathrm{T}}}{\Delta g(t)^{\mathrm{T}}\Delta x(t)}. \tag{17}$$

Search direction in BFGS is selected according to Eq. (15). In the first iteration, the Hessian matrix can be selected as the unit matrix or derivative of the Jacobians matrix. Δw value seen in Eq. (16) is calculated by Eq. (17). Δw is the change of weight at tth iteration [31].

4.3 Scaled conjugate gradient

The scaled conjugate gradient (SCG) algorithm based on conjugate directions was designed to prevent line search, which causes loss of time. All conjugated gradient algorithms need a search at every stage. This search process is very time-consuming in terms of computing. The scaled conjugate gradient algorithm developed by Moller is an algorithm developed to reduce the burden of these over computations. Step size in the SCG algorithm is a function of the second degree of convergence of the error function. This makes it more robust and independent than user-defined parameters. The step size is predicted with different ways of approaches.

$$s_k = \frac{E'(\omega_k + \sigma_k p_k) - E'(\omega_k)}{\sigma_k} + \lambda_k p_k, \tag{18}$$

$$\alpha_k = \frac{g_{k+1}^2 - g_{k+1}^{\mathrm{T}} g_k}{g_k^{\mathrm{T}} g_k}, \tag{19}$$

$$p_{k+1} = -g_{k+1} + \alpha_k p_k, \tag{20}$$

where s is the Hessian matrix approximation. E is the total error function, with E' is the gradient of E. λ and σ are scaling factors. α_k factor and direction of the new search given in Eq. (19) and Eq. (20). The independent update of design parameters at each iteration is a key factor for the success of the algorithm and provides a significant advantage over line search based algorithms [32].

5. Experimental and simulation results

In this study, vibration analyses of trains at three different speeds were performed with the acceleration sensors placed on the rail. Train speeds were predicted by using three types of artificial neural networks algorithms. Fig. 6 shows the real-time estimation results of the vibration by the train at 40 km/h. LMBP, SCGB and BFGS algorithms were used to prediction. The minimum error rate for each activation function combination was determined using the mean squared error (MSE) metric. The MSE measures the proximity of a regression line to a set of points by calculating the average of the squared differences between the points and the regression line. The negative signs are eliminated by squaring the differences, which also gives more emphasis to larger deviations. A low MSE value indicates a high level of accuracy in the forecast as it represents a closer relationship between the predicted values and the actual values.

$$\mathrm{MSE} = \sum_{i=1}^{N} \frac{(o_i - t_i)^2}{2}. \tag{21}$$

Here o_i is the outputs of purposed ANN models, t_i is experimental value and N is total number of data. The regression value "R" quantifies the correlation between the predicted outputs and actual targets. The best prediction result in terms of the number of iterations and response speed was obtained with the LMBP algorithm. Fig. 7 and Fig. 8 shows the estimation results for the train with a speed of 52 km/h and 60 km/h, respectively. The LMBP algorithm carried out a better performance than other algorithms again. Considering the best MSE value is 0 and the best regression value is 1, the MSE and regression values, given in Tab. II, are acceptable for all algorithms. Also, this can be seen from the figures. Nevertheless, in a real-time estimation, it is essential to make fast and accurate predictions. For this purpose, SCGB and BFGS algorithms perform worse prediction and need more time and more iteration to prediction than the LMBP algorithm. Although the vibration that occurs on rail has high amplitude and fluctuation, the LMBP

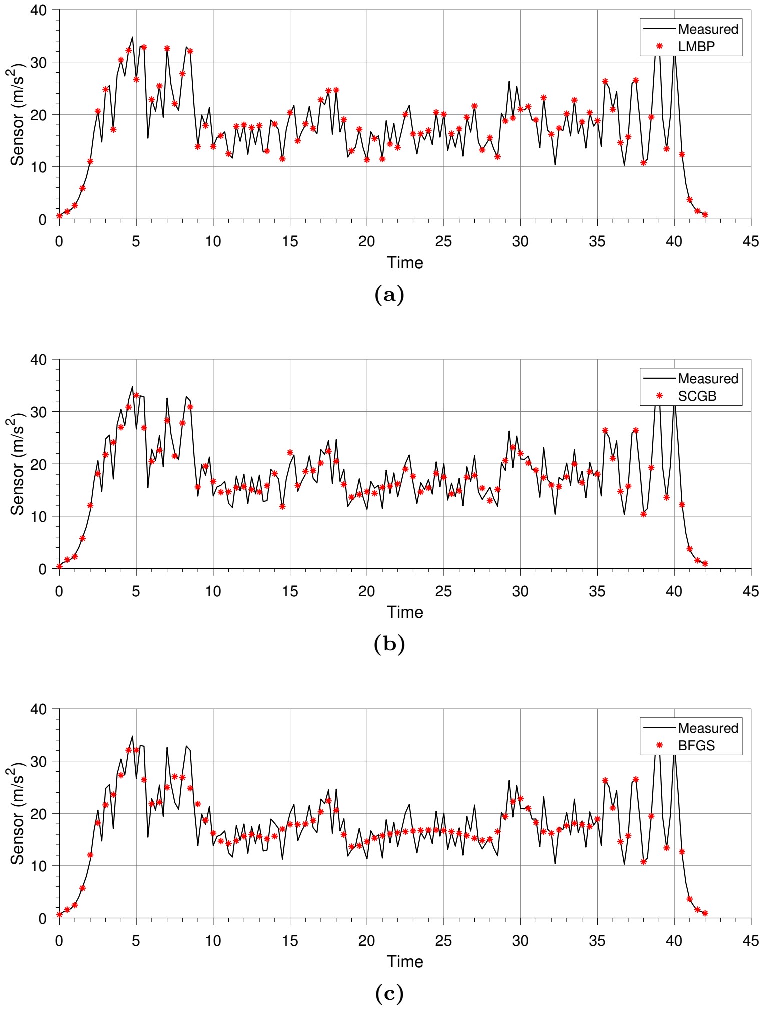

Fig. 6 *Experimental and ANN results for the vibration of the train with 40 km/h. (a) Measured data and LMBP prediction results. (b) Measured data and SCGB prediction results. (c) Measured data and BFGS prediction results.*

algorithm fits almost perfectly to measured data in all vibrations of different speed conditions, and the LMBP algorithm needs less time to predict. In addition, it is seen from the figures that the occurrence time of high amplitude vibrations at slow speed is in an extended period, but the vibration amplitude is low, and the occurrence time al of high amplitude vibrations at high speed is shorter, but the vibration amplitude is higher than the others. For instance, vibration values change between about 12 m/s^2 and 35 m/s^2 at 40 km/h and it takes about 40 seconds. Besides at 60 km/h, vibration values change between about 20 m/s^2 and 140 m/s^2 and it takes about 22 seconds. This situation is expected at different speeds of the train.

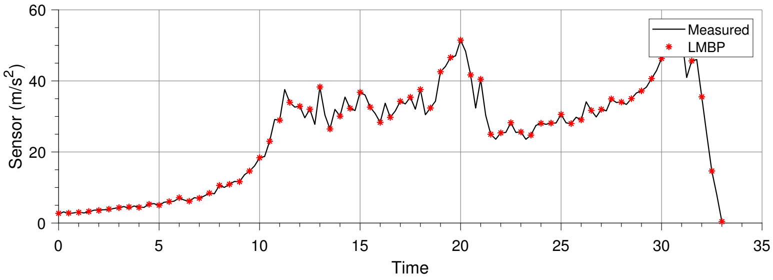

(a)

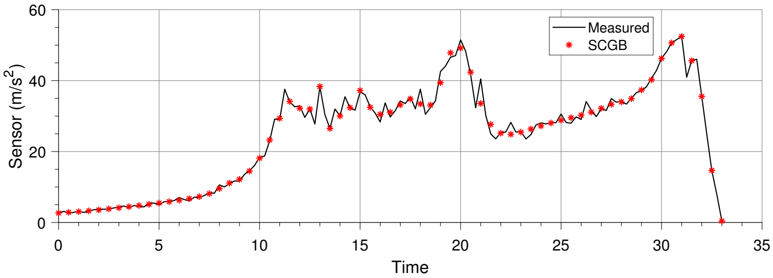

(b)

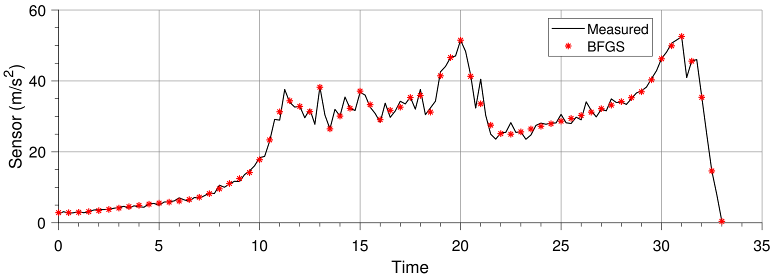

(c)

Fig. 7 *Experimental and ANN results for the vibration of the train with 52 km/h. (a) Measured data and LMBP prediction results. (b) Measured data and SCGB prediction results. (c) Measured data and BFGS prediction results.*

6. Conclusions and discussion

In this study, the neural networks approach was used to predict the speed of a train by analysing the vibrations on the rails. The performance of the neural network was evaluated using the mean squared error (MSE) metric, which measures the difference between the predicted values and the actual values. The regression value, which quantifies the correlation between the predicted outputs and actual targets, was also calculated. An experimental measurement system was established to gather the real-time vibrations caused by a moving train. Three different types

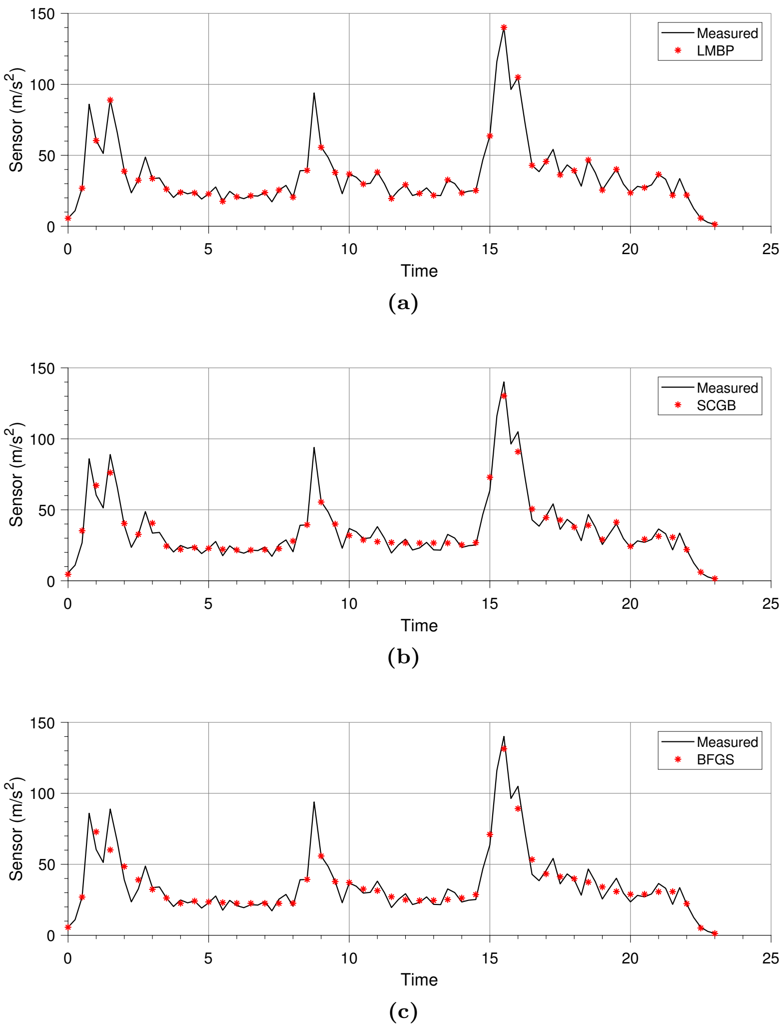

Fig. 8 *Experimental and ANN results for the vibration of the train with 60 km/h: (a) Measured data and LMBP prediction results. (b) Measured data and SCGB prediction results. (c) Measured data and BFGS prediction results.*

of neural network algorithms were employed and compared to determine the optimal neural estimator. The results showed that the LMBP algorithm was able to estimate the speed of the train quickly and accurately from the vibrations, with a low MSE and high regression value.

The goal of this research was to develop a neural predictor for train speeds from rail vibrations, and the LMBP algorithm proved to be effective in achieving this goal in a short amount of time. This means that a low-cost, vibration-based level crossing control system could be installed near crossings, reducing downtime and waiting times for drivers and pedestrians. In the proposed ANN and vibration-

Speed [km/h]	NN Type	s_H	n_I	n_H	n_o	MSE	R
40	LMBP	2	1	20	1	0.00001	0.99997
	SCGB	2	1	20	1	0.01870	0.94239
	BFGS	2	1	20	1	0.02750	0.91398
52	LMBP	2	1	20	1	0.00001	0.99998
	SCGB	2	1	20	1	0.00249	0.99586
	BFGS	2	1	20	1	0.00211	0.99649
60	LMBP	2	1	20	1	0.00001	0.99996
	SCGB	2	1	20	1	0.01030	0.95457
	BFGS	2	1	20	1	0.00968	0.95730

Tab. II *Training parameters of neural networks and MSE and regression values of proposed networks. s_H hidden layer number, n_I number of neurons in input layer, n_H number of neurons in each hidden layer, n_o number of neurons in output layer, MSE mean square errors, R regression.*

based system, the presence and speed of the train can be detected by vibrations on the rails, minimizing cost and human error. The control system + detection system will be installed in a compact structure near the level crossing, instead of far away with long cables.

Today, level crossing control systems are installed near the level crossings, but the sensors and detection systems are located far away and require separate setup and long cables. This has disadvantages such as exposed pole wires at level crossings, the danger of wires breaking, and the cost of separate system installation and maintenance. One of the biggest disadvantages of existing systems is that the barriers close independently of the train speed, causing long waiting times and leading to impatient people trying to cross the level crossing diagonally, resulting in accidents.

In future work, a prototype of a smart level crossing design system will be developed and the artificial neural network approach will be applied. The results of this study will inform the use of the proposed network system to analyse and predict vibration parameters in railway systems under different conditions (different weather conditions, deformations that may occur on the rails, different loading conditions and train types etc.). Advanced intelligent sensor technology can also be utilized in train and railway systems to prevent traffic accidents.

References

[1] Annual statistic of TCDD 2014-2018. [accessed 2020-12-20] *General Directorate Of Turkish State Railways*, 2014–2018. Available from: https://static.tcdd.gov.tr/webfiles/userfiles/files/20142018yillik.pdf.

[2] BAHLOUL K., DEFOSSEZ F., GHAZEL M., COLLART-DUTILLEUL S. Adding technological solutions for safety improvement at level crossings: A functional specification. *Procedia – Social and Behavioral Sciences*, 2012, 48, pp. 1375–1384, doi: 10.1016/j.sbspro.2012.06.1113.

[3] BURDZIK R., NOWAK B. Identification of the vibration environment of railway infrastructure. *Procedia Engineering*, 2012, 187, pp. 556–561, doi: 10.1016/j.proeng.2017.04.414.

[4] ARDIANSYAH H., RIVAI M., NURABDI L.P.E. Train arrival warning system at railroad crossing using accelerometer sensor and neural network. *AIP Conference Proceedings*, 2018, 1977(1), 040029, doi: 10.1063/1.5042999.

[5] LARUE G.S., MISKA M., QIAN G., WULLEMS C., RODWELL D., CHUNG E., RAKOTONIRAINY A. Can road user delays at urban railway level crossings be reduced? evaluation of potential treatments through traffic simulation. *Case Studies on Transport Policy*, 2020, 8(3), pp. 860–869, doi: 10.1016/j.cstp.2020.05.016.

[6] SHARAD S., SIVAKUMAR P.B., ANANTHANARAYANAN V. An automated system to mitigate loss of life at unmanned level crossings. *Procedia Computer Science*, 2016, 92, pp. 404–409, doi: 10.1016/j.procs.2016.07.397.

[7] EDLA D.R., TRIPATHI D., KUPPILI V., DHARAVATH R. Multilevel automated security system for prevention of accidents at unmanned railway level crossings. *Wireless Personal Communications*, 2019, 111, pp. 1707–1721, doi: 10.1007/s11277-019-06952-4.

[8] AL-ZUHAIRI A.S.M. Automatic railway gate and crossing control based sensors & microcontroller. *International Journal of Computer Trends and Technology (IJCTT)*, 2013, 4(7), pp. 2135–2140.

[9] KIRUTHIGA M., DHIVYA M.M., DHIVYA P., YUGAPRI Y.R. Wireless communication system for railway signal automation at unmanned level. *International Journal of Innovative Research in Science, Engineering and Technology*, 2014, 3(1), pp. 592–597.

[10] MOSTAFA S.S., HOSSIAN M., REZA K.J., RASHID G.M. A radio based intelligent railway grade crossing system to avoid collision. *International Journal of Computer Science Issues*, 2010, 6(7), pp. 139–143, doi: 10.48550/arXiv.1109.0077.

[11] BISWAS S., BHUIYAN R.H., HOQUE S., HASAN R., KHAN T.N. Pressure sensed fast response anti-collision system for automated railway gate control. *American Journal of Engineering Research*, 2013, 2(11), pp. 163–173.

[12] AMEEN M. Track vibration based signal system for unattended rail crossing and on track signalling. *International Journal of Computer Sciences and Engineering*, 2017, 5, pp. 181–183, doi: 10.26438/ijcse/v5i8.181183.

[13] KITAMURA S., TERAMOTO M., ITOYA S., FUKUTA Y. Improvement of availability of level crossing system by autonomous decentralized technology. *IEEE 13th International Symposium on Autonomous Decentralized System (ISADS)*, 2017, pp. 143–148, doi: 10.1109/ISADS.2017.35.

[14] BURDZIK R., KONIECZNY Ł., NOWAK B., ROZMUS J. Research on vibration employed for the train traffic control. *Vibroengineering PROCEDIA*, 2017, 14, doi: 10.21595/vp.2017.19237.

[15] XIA H., ZHANG N., DE ROECK G. Dynamic analysis of high speed railway bridge under articulated trains. *Computers and Structures*, 2003, 81(26), pp. 2467–2478, doi: 10.1016/S0045-7949(03)00309-2.

[16] WU T.X., THOMPSON D.J. The effects of track non-linearity on wheel/rail impact. *Proceedings of The Institution of Mechanical Engineers Part F-journal of Rail and Rapid Transit*, 2004, 218(1), pp. 1–15, doi: 10.1243/095440904322804394.

[17] KNOTHE K.L., GRASSIE S.L. Modelling of railway track and vehicle/track interaction at high frequencies. *Vehicle System Dynamics*, 1993, 22(3–4), pp. 209–262, doi: 10.1080/00423119308969027.

[18] XU L., ZHAO Y., Lİ Z., SHİ C., YU Z. Three-dimensional vehicle-ballasted track-subgrade interaction: Model construction and numerical analysis. *Applied Mathematical Modelling*, 2020, 86, pp. 424–445, doi: 10.1016/j.apm.2020.05.007.

[19] GİLARDİ G., SHARF I. Literature survey of contact dynamics modelling. *Mechanism and Machine Theory*, 2002, 37(10), pp. 1213–1239, doi: 10.1016/S0094-114X(02)00045-9.

[20] ZHAI W., CAI Z. Dynamic interaction between a lumped mass vehicle and a discretely supported continuous rail track. *Computers and Structures*, 1997, 63(5), pp. 987–997, doi: 10.1016/S0045-7949(96)00401-4.

[21] UZZAL R.U.A., AHMED W., RAKHEJA S. Dynamic analysis of railway vehicle-track interactions due to wheel flat with a pitch-plane vehicle model. *Journal of Mechanical Engineering*, 2008, 39(2), pp. 86–94, doi: 10.3329/jme.v39i2.1851.

[22] IWNICKI, S. *A Handbook of Railway Vehicle Dynamics. CRC Press*, 2006, doi: 10.1201/9781420004892.

[23] MARQUE, F., MAGALHÃES H., POMBO J., AMBRÓSIO J., FLORES P. A three-dimensional approach for contact detection between realistic wheel and rail surfaces for improved railway dynamic analysis. *Mechanism and Machine Theory*, 2020, 149, 103825, doi: 10.1016/j.mechmachtheory.2020.103825.

[24] ACEITUNO J.F., URDA P., BRIALES E., ESCALONA J.L. Analysis of the two-point wheel-rail contact scenario using the knife-edge-equivalent contact constraint method. *Mechanism and Machine Theory*, 2020, 148, 103803, doi: 10.1016/j.mechmachtheory.2020.103803.

[25] BOZZONE M., PENNESTRÌ E., SALVINI P. Dynamic analysis of a bogie for hunting detection through a simplified wheel–rail contact model. *Multibody System Dynamics*, 2011, 25, pp. 429–460, doi: 10.1007/s11044-010-9233-8.

[26] MONTENEGRO P.A., NEVES S.G.M., CALÇADA R., TANABE M., SOGABE M. Wheel–rail contact formulation for analyzing the lateral train–structure dynamic interaction. *Computers and Structures*, 2015, 152, pp. 200–214, 2015, doi: 10.1016/j.compstruc.2015.01.004.

[27] HAYKIN S., NETWORK N. A comprehensive foundation. *Neural networks*, 2004, 2(2004), 41.

[28] MARQUARDT D.W. An algorithm for least-squares estimation of nonlinear parameters. *Journal of the society for Industrial and Applied Mathematics*, 1963, 11(2), pp. 431–441, doi: 10.1137/0111030.

[29] HAGAN M.T., MENHAJ M.B. Training feedforward networks with the marquardt algorithm. *IEEE transactions on Neural Networks*, 1994, 5(6), pp. 989–993, doi: 10.1109/72.329697.

[30] OZVEREN U. Modeling pem fuel cells with artificial neural networks. *Yildiz Teknik University*, 2006, https://tez.yok.gov.tr/UlusalTezMerkezi/TezGoster?key=-L8ilcwn9ZRRc_YMKxXW1vcUZ2mCxGb-Mt0ENsPYEhbql6CMzgM77LENfZRwAbfF.

[31] SAGIROGLU S., ERLER M., BESDOK E., Applications of neural networks-I in engineering: Artificial neural networks. *Ufuk Publishing, Kayseri*, 2003.

[32] MØLLER M.F. A scaled conjugate gradient algorithm for fast supervised learning. *Neural Networks*, 1993, 6(4), pp. 525–533, doi: 10.1016/S0893-6080(05)80056-5.